

# The patient-specific implant created with 3D printing technology in treatment of a severe open distal humerus fracture with complete loss of the lateral column

Journal of Orthopaedic Surgery  
28(3) 1–8

© The Author(s) 2020

Article reuse guidelines:  
sagepub.com/journals-permissions  
DOI: 10.1177/2309499020960251  
journals.sagepub.com/home/osj



Suriya Luenam<sup>1</sup> , Arkaphat Kosiyatrakul<sup>1</sup>,  
Kantapat Phakdeewisetkul<sup>2</sup>  and Chedtha Puncreobutr<sup>3</sup>

## Abstract

The open distal humeral fracture associated with the major loss of the articular surface and bony structure is a challenging problem for orthopedic surgeons. In this case report, we describe a case of complete missing lateral column of the distal humerus with severe articular destruction of capitellum and lateral trochlear ridge which was treated with the patient-specific implant created with three-dimensional printing technology. Apart from anatomic replacement of the articular surface, the lateral collateral ligament complex and extensor muscle which are the key soft tissue stabilizers of elbow were repaired by reattaching their bony origins to the impacted iliac crest bone graft inside the implant. Due to the favorable result at 2-year follow-up, this modality is a potentially viable surgical option in treating of the severe open distal humeral fracture associated with entire lateral condylar damage.

## Keywords

3D printing, bone loss, capitellum, distal humerus, lateral column, open fracture, patient-specific implant

Date received: 21 March 2020; Received revised 08 August 2020; accepted: 31 August 2020

## Introduction

The open distal humeral fractures made up approximately 2.7% of all open long bone fractures.<sup>1</sup> They were commonly seen in younger individuals involved in higher energy mechanisms. Considerable bone loss sometimes occurs. The radiocapitellar joint transfers up to 60% of the load across the elbow joint.<sup>2</sup> Loss of the lateral condyle would result in 100% of forearm loads crossing the ulnohumeral joint, raising concerns about overload of that cartilage and degenerative arthrosis.<sup>3</sup> The biomechanical study demonstrated that the capitellum also has a role in maintaining the valgus and rotational stability of the ulnohumeral joint.<sup>4</sup> Reconstruction of the capitellar and lateral condylar loss is recommended to restore the elbow kinematics and stability.<sup>2,4</sup> In the present report, we describe the use of a patient-specific implant which was created with three-dimensional (3D) printing

technology to replace the complete loss of the lateral column and severe crushed capitellum. To our knowledge, this is the first report in clinical use of this kind of implant. Written informed consent for publication of the clinical details and

<sup>1</sup> Department of Orthopaedics, Phramongkutklao Hospital and College of Medicine, Bangkok, Thailand

<sup>2</sup> Biomechanics Research Center, Meticuly Co. Ltd., Chulalongkorn University, Bangkok, Thailand

<sup>3</sup> Advanced Materials Analysis Research Unit, Department of Metallurgical Engineering, Faculty of Engineering, Chulalongkorn University, Bangkok, Thailand

## Corresponding author:

Suriya Luenam, Department of Orthopaedics, Phramongkutklao Hospital and College of Medicine, 315 Ratchawithi Road, Bangkok 10400, Thailand.  
Email: luenam\_suriya@yahoo.com



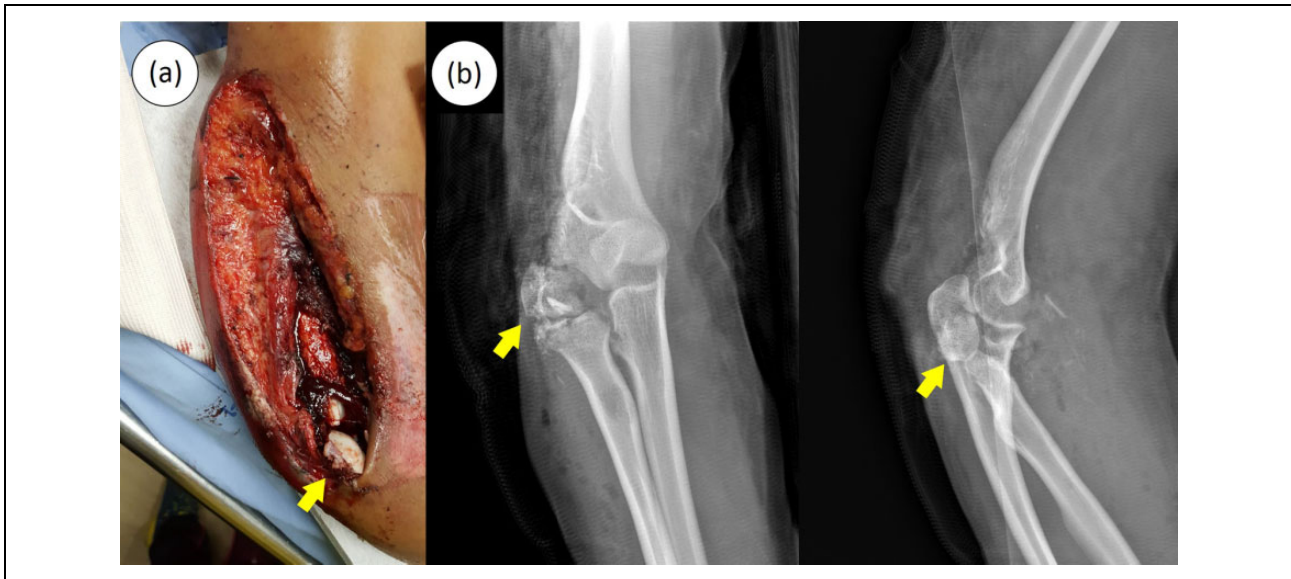


**Figure 1.** (a) A clinical photograph and (b) the plain radiographs in the anteroposterior view (right) and lateral view (left) showing open distal humerus fracture. A crushed osteochondral fragment of the capitellum with minimal joint capsule attachment (yellow arrow).

accompanying images was obtained from the patient. This report has been approved by the Royal Thai Army Medical Department Institutional Review Board (IRBRTA 1037/2563).

### Case presentation

A 25-year-old female patient sustained right elbow injury from the motorcycle accident. The clinical and radiologic examination demonstrated an open fracture of the right distal humerus (Figure 1). The neurovascular status of the right arm was intact. She received the initial wound debridement and lavage from the local hospital prior referral to our department. The computed tomography (CT) scan showed extensive bone loss of the lateral column with destruction of the articular surface of whole capitellum and lateral ridge of the trochlear (Figure 2). The incongruent ulnohumeral joint was noted. Fifty percent of the radial head in the anterolateral and posterolateral quadrants was missing. The patient was taken to the operation theatre for wound reassessment and second debridement in 48 h after the injury. There was the open wound on the lateral aspect of the elbow with circumferential soft tissue contusion. The wound was extended proximally and distally to improve the exposure. The residual contamination and unstable elbow joint were observed. The humeral-sided avulsion of the lateral collateral ligament (LCL) complex and extensor muscle attached to a bony origin was revealed. A 2 cm osteochondral fragment of the capitellum with minimal joint capsule attachment was found. Due to the lack of bleeding, fragility, and unavailable contact border to the remaining joint surface, this fragment was excised and kept in formalin to be used as a template for the subsequent

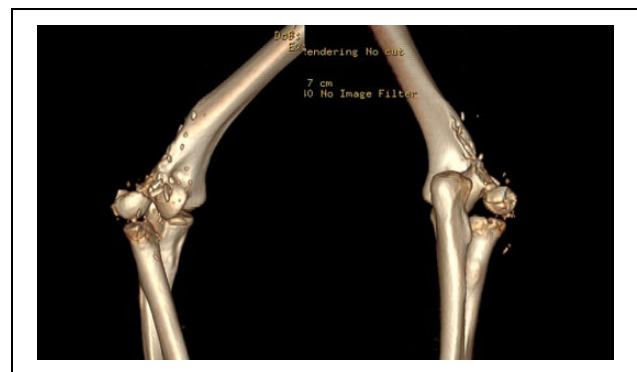


**Figure 2.** A 3D CT reconstruction scan showing the extensive bone loss of the lateral column with destruction of the articular surface of capitellum and lateral trochlear ridge. 3D: three-dimensional; CT: computed tomography.

reconstruction. Following removal of the nonviable tissue and properly irrigation, the external fixator was applied to stabilize the elbow joint, the antibiotic cement beads were placed, and primary wound closure was performed.

Following informative discussion regarding the available treatment options and possible outcomes, the patient would like to be treated with patient-specific implant. The patient had given her explicit consent for this procedure after comprehensive explanation about the details of planning, design, manufacturing process, surgical technique, safety validations and potential complications of the devices.

The implant was designed with a close collaboration between surgical team and engineering team. It was composed of distal articular portion, metaphyseal portion, and side plate. To fabricate the implant, a high-resolution CT scanning (Philips Brilliance 64 CT scanner, Cleveland,

Ohio, USA; voxel size  $0.3 \times 0.3 \times 0.3$  mm, 120 kV, 150 mAs, pitch 0.5) of both distal humeri and elbows was performed and reconstructed into 3D images. The 3D implant model was constructed using the image processing techniques and computer-aided design. The rendered 3D model of the left side was reversed and aligned with the

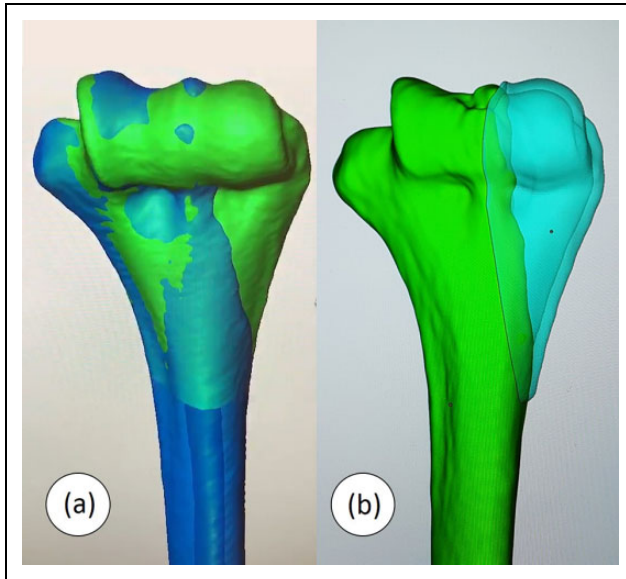


**Figure 3.** The rendered 3D models. (a) The model of affected distal humerus. (b) The model was aligned with a reversed model of normal side by registration the surface of intact portion of the trochlea, metaphysis, and diaphysis to identify correct profile of the articular portion. 3D: three-dimensional.

3D model of the right side by registration the surface of intact portion of the trochlea, metaphysis, and diaphysis to identify correct profile of the articular portion (Figure 3). The additional thickness of cartilage was also augmented to the model using the osteochondral fragment of the capitellum taken from the patient as a guide. The distal articular portion and metaphyseal portion had a hollow body with two transverse bars on the medial side to stabilize the implant on the fracture edge and contain the iliac crest bone graft inside. The inner surface of these portions was roughened by grit-blasting process using aluminum oxide particles to produce an irregularity at 4–7 microns depth. An opening with multiple peripheral suturing holes in the area of lateral epicondyle was created for the attachment of LCL complex. Multiple screw holes were made on the implant for the bone fixation. The side plate was designed conforming to the native anatomy of the distal humerus for total contact in the anterior, posterior, and lateral aspects. The plate length was designed to be 2.5 times higher than the overall fracture to ensure good stability (Figure 4). To determine structural strength of the implant, finite element analysis with ANSYS mechanical software (Ansys Inc., Canonsburg, Pennsylvania, USA) was conducted. It was discovered that the maximal value of the implant stress was well lower than the ultimate strength of 3D-printed titanium alloy. The implant could firmly sustain the load of 200 N which is sufficient for the primary stability.<sup>5</sup>

Upon surgeon's approval of the design, the implant was manufactured by engineering organization (Meticuly Co. Ltd., Chulalongkorn University, Thailand) which is ISO 13485 certified for the development and production of the

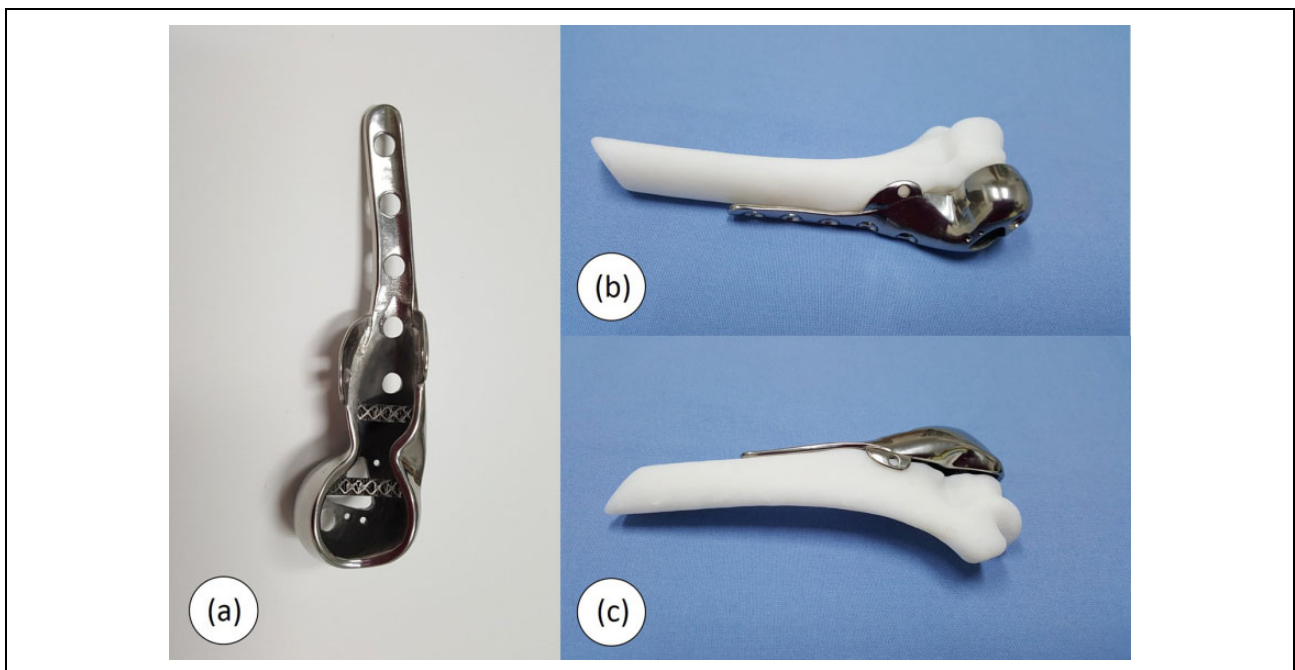


**Figure 4.** The patient-specific implant created with 3D printing technology. (a) The inner aspect. (b) The anterior aspect. (c) The posterior aspect. 3D: three-dimensional.

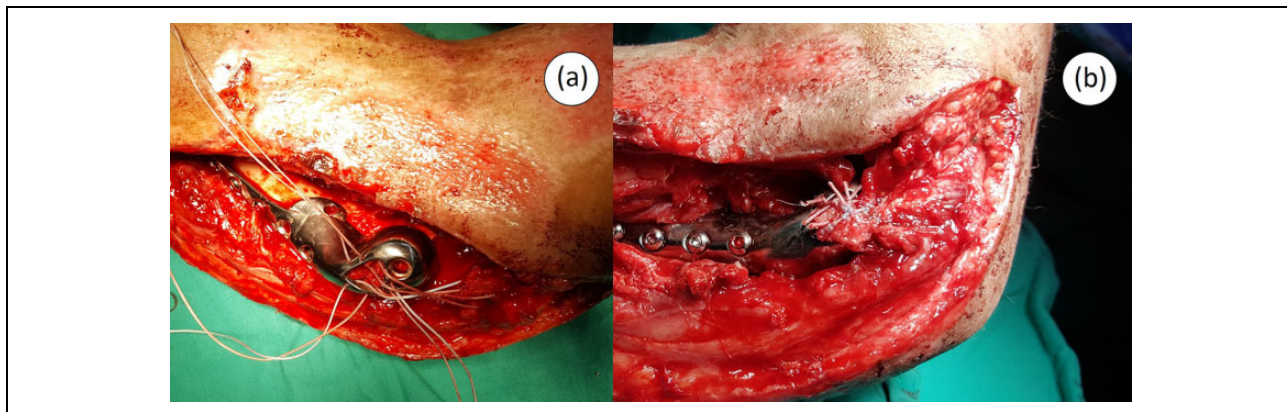


**Figure 5.** Intraoperative photographs. (a) Multiple strands of no. 2 fiber wire were passed through the peripheral holes for supplement of the ligament fixation. (b) The bony end of the LCL complex was passed into the opening of the implant to contact with the underlying bone graft. LCL: lateral collateral ligament.

orthopedic devices. The implant was 3D-printed from medical grade titanium alloy (Ti-6Al-4 V) powder using selective laser melting machine (Mlab cusing 200 R, Concept Laser, Germany). Subsequent post-processing techniques, including surface polishing and sterilization, were performed. The quality control of the 3D printed implant was assessed with a dimensional checking and a surface roughness checking. These processes utilized a 3D measuring microscope, Keyence VR-3200 model, as an instrument. For dimension check, the design of the implant (STL file) was used as a reference to compare with a 3D picture of the actual implant captured from the instrument. A minimum of 90% accuracy is required. For surface roughness check, an area of 1 cm<sup>2</sup> was taken from the 3D captured picture to determine average surface roughness of the implant. The acceptable range is 1–10 microns. In addition, a 3D-printed model of fractured distal humerus made from polycarbonate/acrylonitrile butadiene styrene was used to verify the matching precision as well as the optimal fitment of implant. The biocompatibility and mechanical properties of the titanium implant had been evaluated in line with stringent compliance to ISO 10993 and ASTM F-3001 standards, respectively.

The surgical procedure was performed at 3 weeks after the injury. At this point, the soft tissue was optimized to allow definite treatment and the elbow was free of infection and drainage. The external fixator was removed and the surgical wound was reopened to expose the fracture site. The antibiotic cement was removed and the bone was irrigated with saline. The radial nerve was identified and protected. The patient-specific implant was then inserted having the side plate to fit over the diaphysis and metaphysis. The position was finely adjusted to align the articular portion with the native articular surface. Well conforming of the articular surface was obtained and no additional bone removal was required to fit on the implant. The cavity between the inner surface of the implant (i.e. the surface inside the hollow body at distal articular and metaphyseal portions) and original fractured bone was completely filled

with the corticocancellous iliac crest bone graft. The commercially available screws made from 316 L stainless steel (DePuy Synthes, West Chester, Pennsylvania, USA) were inserted to secure the implant. Five 3.5-mm and one 2.7-mm standard small fragment cortical screws were used at the proximal side with an additional 4.0-mm fully threaded cancellous bone screw used at the distal side.

To reattach the humeral origin of LCL complex, the avulsed bony fragment was passed into the opening to contact with the underlying bone graft. Multiple strands of no. 2 fiber wire were passed through the peripheral holes for reinforcing ligament fixation (Figure 5). Intraoperative fluoroscopy demonstrated a well congruity of the elbow joint through the range of motion. We decided not to do the radial head reconstruction at this point as the concentric reduction was already obtained.

Postoperatively, the elbow was immobilized in a posterior elbow splint at 90°. The splint was removed periodically and the active-assisted range-of-motion of elbow was started to prevent the joint stiffness in 7 days after the surgery. Progressive strengthening program was begun in 6 weeks.

At the latest follow-up, 24 months after surgery, the elbow extension was 15°, flexion was 150°, pronation was 70°, and supination was 90° (Figure 6). Handgrip power of the injured side was 105.7% of the normal side (14.6 kg for injured arm and 13.8 for normal arm). The Mayo Elbow Performance Index was 85 points and the patient-based disabilities of the arm, shoulder, and hand score was 22.5 points. The patient was satisfied with the cosmetic and functional outcomes. The sensation of snapping on the lateral aspect of the elbow occurred once in a while during the first year postoperatively and finally disappeared. The x-rays at the 24-month follow-up demonstrated a well-maintained radiocapitellar and ulno-trochlear joint spaces. No radiolucency around the implant, screw breakage, or change of the implant position was observed (Figure 7). The CT images showed the bridging bony trabeculae of the avulsed bony fragment, iliac crest graft, and native distal humerus (Figure 8).

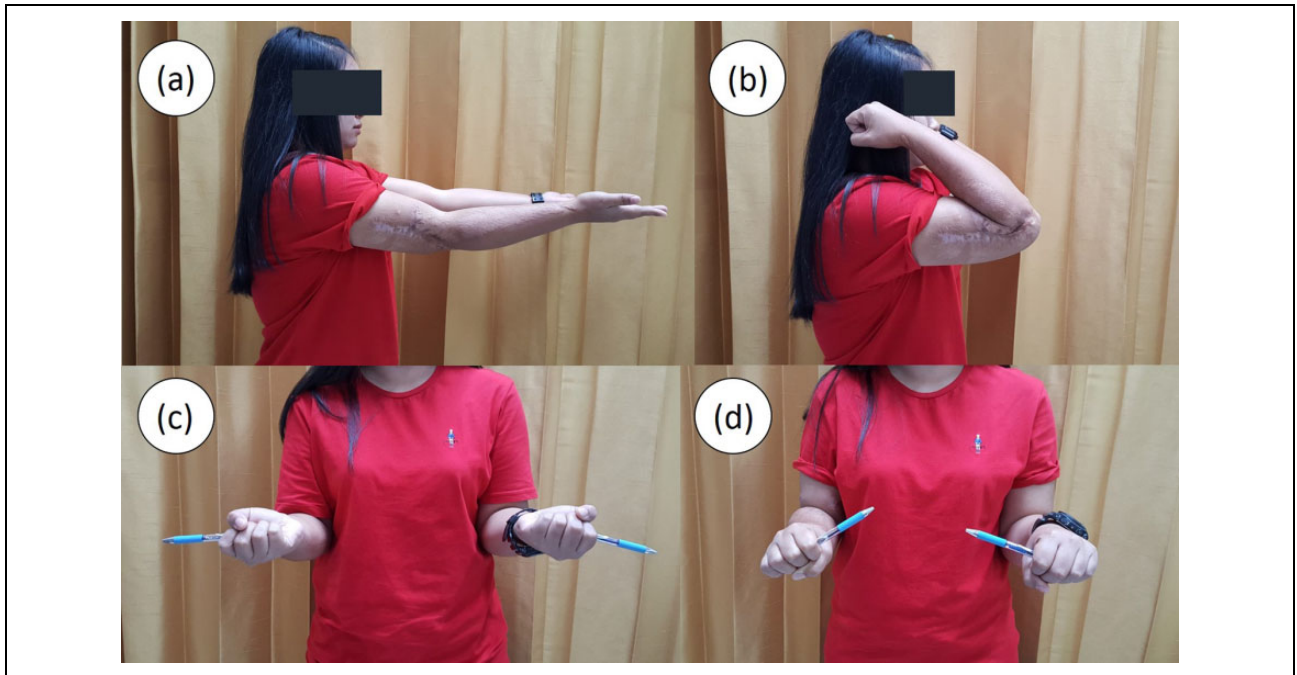


**Figure 6.** Active elbow range of motion at the final clinical follow-up. (a) Active elbow extension, (b) Active elbow flexion, (c) Active supination, and (d) Active pronation.

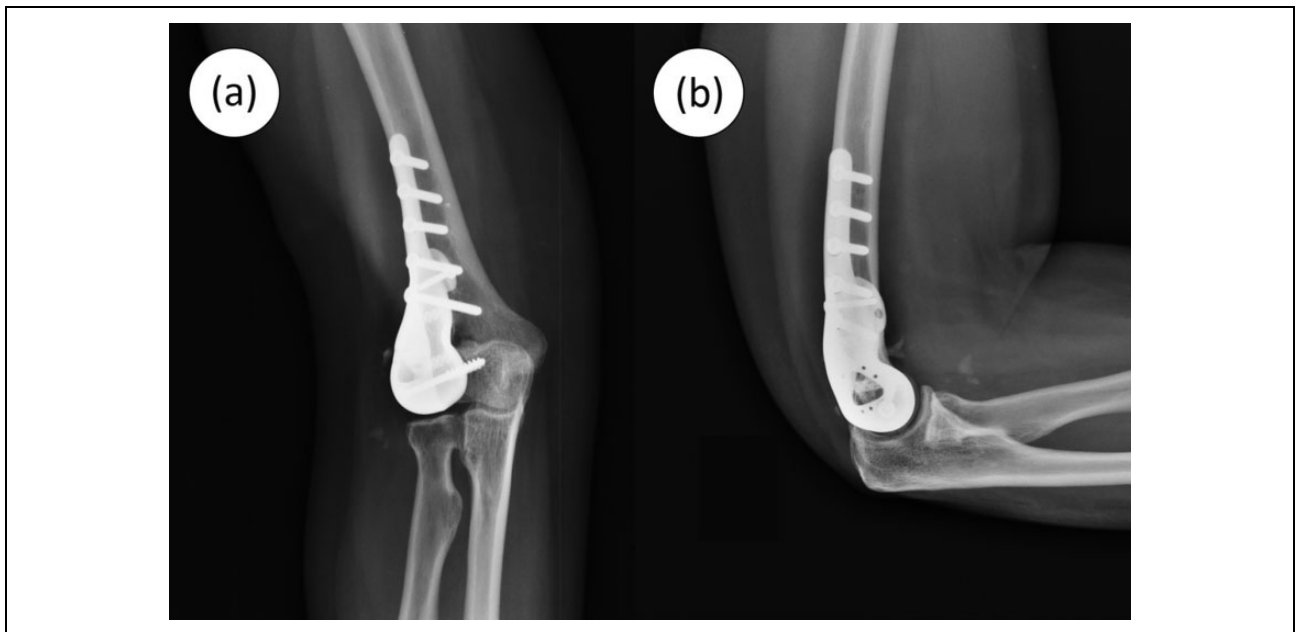


**Figure 7.** The x-rays at 24-month follow-up demonstrated a well-maintained radiocapitellar and ulnotrochlear joint spaces. (a) Anteroposterior view. (b) Lateral view. No radiolucency around the implant, screw breakage, or change of the prosthetic position was observed.

## Discussion

The open distal humeral fracture is a challenging problem for orthopedic surgeons. Such fracture is difficult to treat because of the combined involvement of osseous and soft tissue components.<sup>4</sup> Restoration of adequate elbow function can become even more complicated when the fracture is associated with

the major loss of the articular surface and bony structure.<sup>4,6</sup> In the present report, the patient-specific implant created with 3D printing technology has been used to reconstruct the articular surface and osseous component. The LCL complex and extensor muscle which are the key soft tissue component of the elbow were also anatomically reattached.

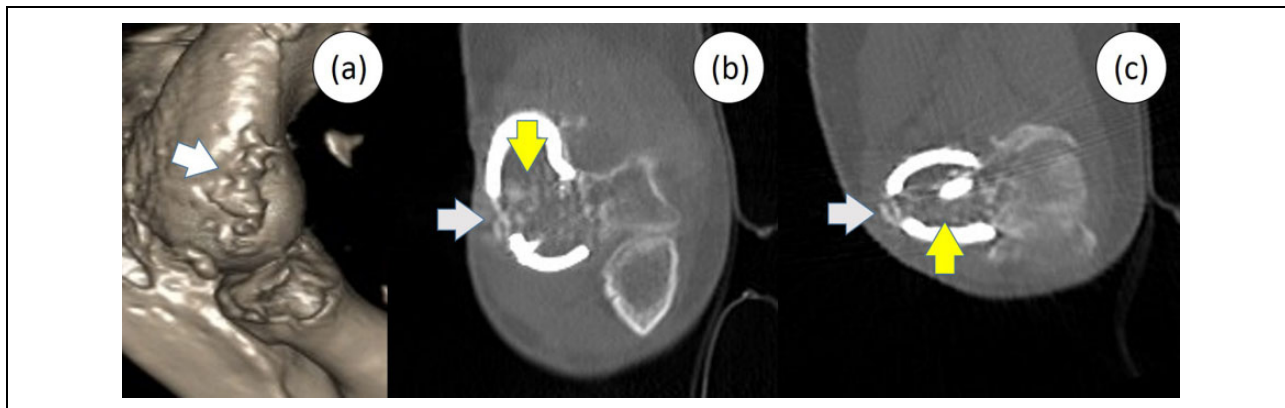


**Figure 8.** The follow-up CT images showed the evidence of bony incorporation of the avulsed bony fragment of LCL complex (white arrow), iliac crest graft (yellow arrow), and native distal humerus. (a) 3D reconstruction. (b) Coronal cut. (c) Axial cut. CT: computed tomography; LCL: lateral collateral ligament; 3D: three-dimensional.

The reconstructive options in management of the distal humeral bone defect are including autograft, allograft, and arthroplasty.<sup>6-11</sup> According to the current literature, the vascularized and nonvascularized autografts were generally used for the juxta- or intra-articular defects which most part of the articular surface still remained.<sup>6,7</sup> Replacement of the distal humerus or total elbow joint with the osteoarticular allograft was also reported. Despite providing a satisfactory functional outcome in several large series, the allograft had a high rate of serious potential complications included nonunion, infection, fracture, allograft resorption, and instability.<sup>8</sup> The total elbow arthroplasty was become increasingly accepted and widespread as a surgical option for elderly patient but the prosthetic longevity in young patients and the postoperative restrictions are of particular concern.<sup>9,10</sup> Distal humeral hemiarthroplasty, in which a commercially humeral component of the unlinked total elbow prosthesis articulates with the native olecranon and radius, was proposed to be used in the young population with the aim to reserve bone stock, avoid significant weight restrictions, and limit loosening.<sup>9-11</sup> However, this requires intact or reconstructible condyles and soft tissue constraints.<sup>10</sup> As the injury in the present case occurred in the dominant arm of the young active patient with massive bone loss and of missing whole lateral condyle, none of the previously described options does not seem to be the ideal treatment.

Based on the symmetry of the human skeleton, we can reverse the 3D images of the normal bone to the contralateral side to create the anatomic prosthesis for the missing part.<sup>12</sup> Using this technique, the tailor-made prostheses for several bones and joints have been previously reported.<sup>13,14</sup> The recent biomechanic study in the cadaveric arms demonstrated that the reverse-engineered distal humeral hemiarthroplasty prostheses did not reproduce the same contact pattern as the native joints, possibly because the prostheses were designed based on distal humeral osseous anatomy from the CT images which is lacked inclusion of

the cartilage thickness.<sup>15</sup> For this reason, the authors utilized an osteochondral fragment of the capitellum which was obtained from the surgical debridement to guide for the appropriate morphologic shape and dimension of the surface of the articular portion. Intraoperatively, the conforming surface of the implant with the native bone facilitated the intraoperative placement and aided for accurate positioning. In the present case, the remaining native articular surface could be preserved and no additional bone removal is required to fit on the implant.

Apart from the bony injury, the open distal humeral fracture always has the associated soft tissue injury.<sup>2</sup> The present case also had the insufficiency of LCL complex which is one of the primary stabilizers of the elbow joint.<sup>16</sup> Anatomic reattachment of the avulsed LCL bony fragment was unfeasible because of the entire condyle bone loss. Concern existed regarding ligament healing if LCL complex was secured directly with the metal implant. To obtain the optimal repair with bone to bone healing, an undersurface of the implant was designed to provide a space for impaction of the iliac crest autologous bone graft. The avulsed bony fragment was passed into a lateral opening of the implant to connect with the underneath impacted graft. Impaction bone grafting procedure was previously described in hip replacement for managing deficient bone stock. Graft incorporation was documented with such procedure in the experimental and retrieval studies.<sup>17,18</sup> The healing and integration of the avulsion fragment, bone graft, and native distal humerus of the present case was evidenced by the follow-up CT images. The occasionally sensation of snapping on lateral aspect of the elbow is probably because of radiocapitellar instability from the loss more than one-third of radial head or impingement of the radial head fracture edge with the adjacent bone or soft tissue.<sup>19</sup> This symptom was spontaneously resolved during follow-up perhaps due to further strengthening of the ligament and muscle and remodeling of the radial head.

In the present case, the implant was fabricated from medical-grade titanium alloy (Ti-6Al-4 V) instead of other materials, such as cobalt-based alloy or stainless steel, because of its relatively lower elastic modulus which is more efficient in interface stress transfer.<sup>20</sup> This is likely to reduce stress shielding, enable better graft loading, encourage graft incorporation, and prevent subsequent graft resorption.<sup>21</sup> Furthermore, the surface inside the hollow body at distal articular and metaphyseal portions of the implant that was planned to be in contact with bone graft was specifically roughened by grit-blasting process. This grit-blasting process provides a roughened surface of 4–7 microns that is sufficient to enhance osseointegration of bone graft onto the implant surface (bone on-growth), improving the likelihood of implant survivorship.<sup>22</sup> The use of reconstruction cage which had similar surface design with impaction bone grafting demonstrated the encouraging mid-term results with low failure rate in managing severe complex uncontained acetabular bony defects.<sup>23</sup>

Based on the principle of biologic fixation, initial rigid stability of the implant is required for long-term osteointegration.<sup>24</sup> To obtain primary stability, screw fixation of the implant to host bone was planned. As the titanium screws were not available, additional process of manufacturing the titanium screws would be complex and time-consuming, which was not suitable in this semi-urgent situation. The commercially available screws made from 316 L stainless steel were used to secure the implant. We were aware that internal fixation with multiple metal implants that dissimilar in electrochemical potential had been concerned about the occurrence of galvanic corrosion which might subsequent cause failure of the fixation and of bone healing.<sup>25</sup> However, numerous laboratory, animal, and human studies have shown that combination of dissimilar screws and plates did not accelerate the corrosion than the single-material constructions, indicating comparable clinical safety.<sup>25,26</sup> In the present case, combination of titanium and stainless steel implants did not show any negative effect on fixation stability or bone incorporation at 2-year follow-up.

Although the patient-specific implant created with 3D printing technology demonstrated the encouraging results in the difficult-to-treat cases in which conventional treatments are not an option, the regularity requirement in application is one of the reasons that the surgeons hesitate to use of such implants.<sup>27</sup> The regulations are variable among counties.<sup>28</sup> In the United States, it is required to meet standards for good manufacturing practices under the Food and Drug Administration (FDA)'s quality system regulation. However, FDA allows for a patient-centered approach: the special custom device exemption act permits the use of custom-made devices for patients with special needs with a rare and unique pathology for which no conventional treatment is available. In the European countries, these devices fell into EU Medical Device Directive annex XIII. Willemsen et al. described a useful guideline of in-house development pathways and technical files, which may aid

the physicians for regulatory and legal purposes in the semi-urgent situation.<sup>27</sup> According to the current regulations of patient-specific device in our country, there is no specific requirements for application of patient-specific implants. The surgeon is responsible for ethical considerations and for providing extensive information to the patient and acquiring their consent.

## Conclusion

The patient-specific implant created with 3D printing technology provided satisfactory functional result in treatment of a severe open distal humerus fracture with complete loss of the lateral column. This could also be a useful treatment for other locations and other patterns of the massive osteoarticular humeral defect as the implant can be designed to accommodate to the native anatomy and allow the ligament repair or reconstruction. Further research with a larger number of cases is needed to determine the effectiveness of such implant.

## Acknowledgments

The authors thank Dr Suwicha T Chitpatima for editorial assistance.

## Declaration of conflicting interests

The author(s) declared no potential conflicts of interest with respect to the research, authorship, and/or publication of this article.

## Funding

The author(s) received no financial support for the research, authorship, and/or publication of this article.

## ORCID iD

Suriya Luenam  <https://orcid.org/0000-0002-0126-9218>  
Kantapat Phakdeewisetkul  <https://orcid.org/0000-0002-3073-2240>

## References

1. Court-Brown CM, Rimmer S, Prakash U, et al. The epidemiology of open long bone fractures. *Injury* 1998; 29: 529–534.
2. Halls AA and Travill A. Transmission of pressures across the elbow joint. *Anat Rec* 1964; 150: 243–247.
3. Sabo MT, Shannon HL, Deluce S, et al. Capitellar excision and hemiarthroplasty affects elbow kinematics and stability. *J Shoulder Elbow Surg* 2012; 21: 1024–1031.
4. Min W, Anwar A, Ding BC, et al. Open distal humerus fractures—review of the literature. *Bull NYU Hosp Jt Dis* 2010; 68: 257–261.
5. Kudo T, Hara A, Iwase H, et al. Biomechanical properties of orthogonal plate configuration versus parallel plate configuration using the same locking plate system for intra-articular distal humeral fractures under radial or ulnar column axial load. *Injury* 2016; 47: 2071–2076.

6. Kouvidis GK, Chalidis BE, Liddington MI, et al. Reconstruction of a severe open distal humerus fracture with complete loss of medial column by using a free fibular osteocutaneous graft. *Eplasty* 2008; 8: e24.
7. Zha Y and Xie-Yuan J. Treatment of delayed humeral intercondylar fracture associated with severe bone defects by iliac bone autografting reconstruction. *J Clin Case Rep* 2016; 6: 693.
8. Kharrazi FD, Busfield BT, Khorshad DS, et al. Osteoarticular and total elbow allograft reconstruction with severe bone loss. *Clin Orthop Relat Res* 2008; 466: 205–209.
9. Rangarajan R, Papandrea RF, and Cil A. Distal humeral hemiarthroplasty versus total elbow arthroplasty for acute distal humeral fractures. *Orthopedics* 2017; 40: 13–23.
10. Mighell MA, Frankle MA, and Mulieri PJ. Elbow arthroplasty for distal humeral fractures-technique, pearls, and pitfalls. *Oper Tech Orthop* 2010; 20: 38–47.
11. Phadnis J, Watts AC, and Bain GI. Elbow hemiarthroplasty for the management of distal humeral fractures: current technique, indications and results. *Shoulder Elbow* 2016; 8: 171–183.
12. Luenam S, Vongvanichvathana A, Kosiyatrakul A, et al. Matching precision of the reverse contralateral radial head in generating of the individualized prosthesis from the surface registration in tuberosity-neck and in tuberosity-diaphysis. *J Orthop Surg (Hong Kong)* 2019; 27(1): 2309499018821774.
13. Punyaratabandhu T, Lohwongwatana B, Puncreobutr C, et al. A patient-matched entire first metacarpal prosthesis in treatment of giant cell tumor of bone. *Case Rep Orthop* 2017; 2017: 4101346.
14. Luenam S, Kosiyatrakul A, Hansudewechakul C, et al. The patient-specific implant created with 3D printing technology in treatment of the irreparable radial head in chronic persistent elbow instability. *Case Rep Orthop* 2018; 2018: 9272075.
15. Willing R, Lapner M, King GJ, et al. In vitro assessment of the contact mechanics of reverse-engineered distal humeral hemiarthroplasty prostheses. *Clin Biomech (Bristol, Avon)* 2014; 29: 990–996.
16. Camp CL, Fu M, Jahandar H, et al. The lateral collateral ligament complex of the elbow: quantitative anatomic analysis of the lateral ulnar collateral, radial collateral, and annular ligaments. *J Shoulder Elbow Surg* 2019; 28(4): 665–670.
17. Ullmark G and Obrant KJ. Histology of impacted bone-graft incorporation. *J Arthroplasty* 2002; 17(2): 150–157.
18. Linder L. Cancellous impaction grafting in the human femur: histological and radiographic observations in 6 autopsy femurs and 8 biopsies. *Acta Orthop Scand* 2000; 71(6): 543–552.
19. Beingessner DM, Dunning CE, and Beingessner CJ. The effect of radial head fracture size on radiocapitellar joint stability. *Clin Biomech (Bristol, Avon)* 2003; 18: 677–681.
20. Head WC, Bauk DJ, and Emerson Jr RH. Titanium as the material of choice for cementless femoral components in total hip arthroplasty. *Clin Orthop Relat Res* 1995; 311: 85–90.
21. Ding H, Mao Y, and Yu B. The use of morselized allografts without impaction and cemented cage support in acetabular revision surgery: 4 to 9 year follow up. *J Orthop Surg Res* 2015; 10: 77.
22. Boyan BD, Lohmann CH, Dean DD, et al. Mechanisms involved in osteoblast response to implant surface morphology. *Annu Rev Mater Res* 2001; 31: 357–371.
23. Hosny HAH, El-Bakoury A, Fekry H, et al. Mid-Term results of graft augmentation prosthesis II cage and impacted allograft bone in revision hip arthroplasty. *J Arthroplasty* 2018; 33: 1487–1493.
24. Albrektsson T, Brånemark PI, Hansson HA, et al. Osseointegrated titanium implants. Requirements for ensuring a long-lasting, direct bone-to-implant anchorage in man. *Acta Orthop Scand* 1981; 52: 155–170.
25. Høl PJ, Mølster A, and Gjerdet NR. Should the galvanic combination of titanium and stainless steel surgical implants be avoided? *Injury* 2008; 39: 161–169.
26. El-Zayat BF, Ruchholtz S, and Zettl R. Results of titanium locking plate and stainless steel cerclage wire combination in femoral fractures. *Indian J Orthop* 2013; 47: 454–458.
27. Willemsen K, Nizak R, Noordmans HJ, et al. Challenges in the design and regulatory approval of 3D-printed surgical implants: a two-case series. *Lancet Digital Health* 2019; 1: e163–e171.
28. Choy WJ and Mobbs RJ. Current state of 3D-printed custom-made spinal implants. *Lancet Digital Health* 2019; 1: e149–e150.